Evaluating the effect of tire parameters on required drawbar pull energy model using adaptive neuro-fuzzy inference system

Taghavifar, H. & Mardani, A.

Original citation & hyperlink:
Taghavifar, H & Mardani, A 2015, 'Evaluating the effect of tire parameters on required drawbar pull energy model using adaptive neuro-fuzzy inference system' Energy, vol. 85, pp. 586-593.
https://dx.doi.org/10.1016/j.energy.2015.03.072

DOI 10.1016/j.energy.2015.03.072
ISSN 0360-5442
ESSN 1873-6785

Publisher: Elsevier

This is the pre-print version of the paper published by Journal of Energy

Evaluating the effect of tire parameters on required drawbar pull energy model using adaptive neuro-fuzzy inference system

Authors:

Hamid Taghavifar*, Aref Mardani

Affiliation:

Department of Mechanical Engineering, Urmia University, Urmia, Iran

E-mail: ha.taghavifar@urmia.ac.ir

hamid.taghavifar@gmail.com

Abstract

Determination of the required energy for drawbar pull of agricultural tractors plays a significant role in the characterization of the quality of tractors during different operations. Assessment of the effect of some tire parameters on drawbar pull energy was performed utilizing a single-wheel tester in a soil bin facility. To this aim, the potential of a global searching soft computing approach (i.e. adaptive neuro-fuzzy inference system) with various membership functions was evaluated. The tire parameters of velocity at three levels of 0.8, 1 and 1.2 m/s, wheel load at three levels of 2, 3 and 4 kN and slippage at three levels of 8, 12 and 15% were applied to single-wheel tester while four installed load cells were responsible for the measurement of drawbar pull. It was concluded that drawbar pull energy is a direct function of wheel load, velocity and slippage. Hence, the greatest value of 1.056 kJ corresponded to the wheel load of kN, slippage of 15% and velocity of 1.2 m/s. The outperforming model yielded mean square error and coefficient of determination values of 0.00236 and 0.995, respectively.

Keywords: Artificial intelligence; ANFIS; Energy; Drawbar pull; Soil bin

1. Introduction

Much advancement in farming techniques and tools has been manifested since the increased demand for food owing to the increased global population. Employment of agricultural tractors for pulling various farming tools is therefore unavoidable in mechanized agriculture. Hence, investigations must be carried out to reach the optimal maxima of drawbar pull to perform different farming operations. Drawbar pull of a tractor is directly a function of the interaction between tire and soil at the soil-tire interface. During soil-wheel interaction, the soil beneath the tire is partially compacted leading to improved soil resistance and simultaneous tire is a substantial source of power loss. Studies indicate that about 20–55% of the power delivered to the tractor drive wheels is wasted in the tire–soil interaction. This energy is not only wasted but the resulting soil compaction created by a portion of this energy may be detrimental to crop production [1]. The detrimental effect of the soil physical characteristics as well as tire parameters on tractive parameters such as rolling resistance (and therefore energy dissipation) has also been investigated on a sandy clay loam soil in an indoor tire traction testing facility [2]. Accordingly, this loss of energy by pneumatic tires has encouraged investigators to search for operational parameters that could improve the net traction ratio and tractive efficiency.

There are studies documented in literature concerned with the evaluation of net traction of driving wheels [3]. It is known that the drawbar pull, travel reduction (slip), and rolling resistance are the main criteria to describe the traction behaviour of off road vehicles wherein the drawbar pull is influenced by the traction conditions such as soil and the tire parameters [4]. In order to assess the relationship between travel reduction and tractive performance, the experimental tests were conducted in a soil bin wherein an artificial neural network (ANN) model with a back propagation learning algorithm was developed to predict the tractive performance of a driven tire in a clay loam soil under varying operating and soil conditions [5]. In Ref. [6] the tire driving torque, drawbar pull, tire sinkage, position of tire lug, travel distance of the single wheel-tester and tire revolution angle were measured and it was observed that relationships of slip vs. sinkage and drawbar pull vs. slip showed high correlation. A comprehensive study was also undertaken to define the traction and tractor performance as affected by different tire parameters such as slip and forward speed [7]. The study led to the understanding on maximizing the fuel efficiency of the engine and drivetrain, maximizing the tractive advantage of the traction devices, and selecting an optimum travel speed for a given tractor-implement system. Different single wheel testing equipment was used to investigate tire performance and different mathematical methods were used to process the measured data [8]. In a study, field experiments on off-road vehicle traction and wheel–soil interactions were performed on sandy and loess soil surfaces and the tests were carried out at nominal and reduced inflation pressures and at three vehicle loading levels: empty weight, loaded with 3.6 and 6.0 t mass (8000, 11,600 and 14,000 kg, respectively). Drawbar pull was quantified with a load cell, attached to the rear of the test vehicle and the front of the towed vehicle which provided drawbar pull to the test vehicle [9]. Tractive performance data were collected in the soil bins at the USDA-ARS National Soil

Dynamics Laboratory (Auburn, Ala.) for two tire types at two levels of travel reduction and three tire inflation pressure levels [10].

The complex nature of soil-tire interaction and the lack of any closed form mathematical description of the phenomena have driven researchers to employ stochastic soft computing techniques to successfully perform nonlinear modeling [11]. For the estimation of the rolling resistance of wheel as affected by velocity, tire inflation pressure, and normal load acting on wheel inside the soil bin facility, a 3-10-1 feed-forward Artificial Neural Network (ANN) with back propagation (BP) learning algorithm was used with a great report on the ability of ANN to deal with the prediction of rolling resistance as an important index of energy dissipation [12]. Similar studies for the prediction of tractive parameters using ANN [13] and fuzzy logic system in a soil bin testing facility were performed [14]. Fuzzy logic system has also been developed to deal with the effects of tire parameters on contact area and contact pressure as influential parameters on the soil deformation an therefore energy loss [15]. In Ref. [16] a method for extracting data on regolith online with a planetary exploration micro-rover was introduced given that the method used a trained neural network successfully to map engineering data from an instrumented chassis to estimates of regolith parameters. Energy dissipation through the rolling resistance of off-road vehicles has been modeled using soft computing approaches by support vector regression [17] and prediction of energy efficiency by the use of artificial neural network [18] with the reports on the robustness of these methods. A multi-criteria based optimization method was also adopted to assess the minimization of energy loss of off-road vehicles [19].

Although the shared purpose of researchers is to predict the soil-wheel interactions, the stochastic nature of soil-wheel interactions and their dependence on several parameters interrupt the development of a general mathematical and classical-based model. However, this difficulty can be solved by use of nonlinear and complex calculation methods such as adaptive network-based fuzzy inference system (ANFIS). The main benefit of these models is that they do not need identifying functional relationships a priori; they self-organize their structure and adapt it in an interactive manner learning the underlying relationship(s) [20]. An adaptive network is a multilayer feed forward network in which each node performs a particular function on giving the input to the network [21].

To the best knowledge of the authors, there is no study dedicated to the investigation of drawbar pull energy of driving wheels utilizing a single-wheel tester in soil bin facility and also applying ANFIS modeling tool. The main objective of this investigation is (i) to assess the influence of velocity, wheel load and slippage on drawbar pull energy and (ii) to prognosticate the objective parameter by the global search exploration approach of ANFIS. This paper is thus organized as following. In section 2, experimental data acquisitioning phase is described. In section 3, ANFIS approach is briefly discussed and the employed structures are introduced. In section 4, the results and discussions are presented. Section 5 is dedicated to the concluding remarks.

2. Experimental data acquisitioning

Aiming to obtain the required data, it is helpful to perform the experiments in controlled conditions which are provided in soil bin testing facility equipped with a single-wheel tester. The soil bin facility consisted of a bin chassis, carriage, controlling consoles and powering unit. A single-wheel tester is typically mounted on the carriage compartment to perform various experiments. The capacious soil bin of Department of Agricultural Machinery of Urmia University (Urmia, Iran) is 24 m in length, 2 m wide and 1 m deep and this relatively substantial size reduces boundary effects. Comprised of a single wheel-tester, a general-purpose carriage, a control panel, and soil preparation equipment, the system is appropriate for conducting soil-wheel experiments. The carriage measures 1.90 m ×2m× 0.95 m and weighs 485 kg. At two sides of the soil bin, steel rails facilitated the motion of the carriage and attached single wheel-tester along the soil bin. An electric motor with the power of 22 kW at a nominal rotational speed of 1457 rpm with a roller chain system pulled the carriage along the soil bin. For rotational speed of the motor, a SV220IS5-2NO, 380VAC model of LG inverter (LG, South Korea) was used with an information display panel that provided speed control for the carriage and with application of chain system enabled the forward and reverse movement of the carriage.

The single wheel tester consisted of a main hub to accommodate the various sizes of tires, lifting arms, a loading platform and a power transmission system. The U-shaped frame of the wheel tester had the ability to rotateabout its vertical axis for varying the steer angle of the test tire. An L-shaped frame connected the wheel-tester and carriage. A three-phase, 5 kW, 1430 rpm induction motor was used to make driving power for the wheel. The speed of the motor was reduced by gear box (7.5:1) then reduced by a gear reduction unit (4.5:1) and the final reduction ratio was 33.75:1. The soil bin facility and single-wheel tester are shown in Fig. 1. The tire was directly driven by the electric motor. An electric motor and an inverter were used to impose desired rotational speed for the test tire. The difference between the peripheral speed for the tire on the wheel-tester and the carriage travel speed provided desired slippage levels. The tire used for the experiments was a 220/65R21 driving tire. The tire tester hub and the L-shaped frame of the carriage are connected by a four-bar mechanism each of which is horizontally parallel. The four-bar mechanism maintains the horizontal position of the load cells for determining net traction. This mechanism provides sufficient strength of connections in pivots and following ground unevenness for the tester during traversing. Four load cells were located on four parallel arms to measure the longitudinal forces to determine traction force and another load cell was located on a bolt power of wheel to measure the vertical load on the wheel. The vertical load cell transmitted data to a separate digital indicator. The load cells sent data to a Bongshin model BS722 digital indicator and from an output digital indicator by RS-232 port to a data logger. In addition to synchronization, data were sent by USB port to a computer and then were stored. The general flow of the experiments and soil properties and are given in Table 1 and Table 2, respectively.

The longitudinally oriented load cells yield the net traction. Assessment of drawbar pull energy was based on direct measurement of net traction and quantifying the waste power as follows:

$$P = \frac{DP \times dx}{dt} = DP \times V \tag{1}$$

where P is output power, DP is drawbar pull (N) and V is velocity (m/s). The loss of power is then used to calculate the loss of energy by knowing the time of wheel traversing as:

$$W = \int P dt \tag{2}$$

Hence,

$$W = \int DPV dt \tag{3}$$

Therefore the measurement of drawbar pull and forward velocity are required to quantify the energy.

3. Adaptive neuro-fuzzy inference system (ANFIS)

ANFIS is a global search soft computing technique that has been successfully used for mapping an input-output relationship based on available data sets. It is based on the first order Takagi-Sugeno fuzzy inference system proposed by Jang [22] and it uses neural network learning algorithms and fuzzy reasoning to map an input space to an output space. With the capability to combine the numeric power of a neural system with the verbal power of a fuzzy system, ANFIS has been found to be promising in modeling problems. The model works on a set of linguistic rules developed using expert knowledge. The fuzzy rule base of the ANFIS model is set up by combining all categories of variables. A typical ANFIS structure, which can be seen in Fig. 2, includes 6 layers. The first layer contains membership functions (MFs). The most common MF involves triangular and bell-shaped functions.

A typical rule set with two fuzzy IF–THEN rules for the first-order Sugeno fuzzy model is the following:

- Rule 1: IF $x=A_1$ and $y=B_1$ THEN $f= p_1 x + q_1 y + r_1$
- Rule 2: IF $x=A_2$ and $y=B_2$ THEN $f= p_2 x + q_2 y + r_2$

Including input layer into considerations, ANFIS structure includes six layers. The procedure is described as follows.

- First layer is the input layer which has n nodes where n is the representative of the system inputs number.
- Second layer is the fuzzification in which each node represents a membership function. The node function of a node i can be expressed by:

$$O_i^1 = \mu_{A_i}(x), \quad \text{i=1,2}$$
$$O_i^1 = \mu_{B_{i=2}}(y), \quad \text{i=3,4} \tag{4}$$

- Third layer provides the strength of the rule by means of multiplication operator in each node.

$$O_i^2 = \mu_{A_i}(x)\mu_{B_i}(y), \quad \text{i=1,2} \tag{5}$$

- Fourth layer is the normalization layer which normalizes the firing strength of the rules according to the following equation:

$$\overline{z_i} = \frac{z_i}{z_1 + z_2}, \quad \text{i=1,2} \tag{6}$$

- Fifth layer consists adaptive nodes each of which computes a linear function whose coefficients referred to as consequent parameters are adapted by using the error function of the feed-forward neural network [23].

$$\overline{z_i} f_i = \overline{z_i}(p_i x + q_i y + r_i) \tag{7}$$

- Sixth layer has a single node which is the sum of the inputs of the nodes in the fifth layer. The output f is computed as follows:

$$f = \overline{z_1} f_1 + \overline{z_2} f_2 = \frac{z_1 f_1 + z_2 f_2}{z_1 + z_2} \tag{8}$$

ANFIS relates the gradient descent methodology to describe the optimal conditions for tuning the membership functions to map input variables to output variables. The main ideology of ANFIS is based on the back-propagation gradient descent methodology that quantifies error signals repetitively from the output layer backward to the input nodes (iteration). However, we used a hybrid method of the gradient descent and the least-squares method to find optimal learning parameters.

Data were split and shuffled into 80% training and 20% testing portions to avoid the overfitting drawback. Various membership functions of l: Built-in membership function composed of the difference between two sigmoidal membership functions (dsigmf), 2: Generalized bell-shaped built-in membership function (gbellmf), 3: Π-shaped built-in membership function (pimf), 4: Triangular-shaped built-in membership function (trimf), 5: Trapezoidal-shaped built-in membership function (tramf), 6: Gaussian curve built-in membership function (gaussmf), and 7: Sigmoidally shaped built-in membership function (sigmf), were adopted in the modeling implementations.

In modeling disciplines, it is absolutely essential to assess the performance of developed models by various statistical criteria. The mean square error (MSE) and the coefficient of determination (R^2) are introduced for analysis of model quality as described below, respectively.

$$MSE = \frac{1}{n}\sum_{i=1}^{n}(Y_{predicted} - Y_{actual})^2 \tag{9}$$

$$R^2 = \frac{\sum_{i=1}^{n}(Y_{predicted} - Y_{actual})^2}{\sum_{i=1}^{n}(Y_{predicted} - Y_{mean})^2} \tag{10}$$

where Y_{actual} and $Y_{predicted}$ are measured and predicted values of the developed models, respectively.

4. Results and discussion

As seen from Fig. 3, the greatest drawbar pull energy (DPE) value of 1.056 kJ corresponded to the treatment of wheel load at 4 kN, slippage at 15% and velocity at 1.2 m/s. Additionally, the lowest DPE value of 0.368 kJ corresponded to the treatment of wheel load at 2 kN, slippage at 8% and velocity at 0.8 m/s. As appreciated from Fig. 3, increased slippage led to an increase in drawbar pull enegy where the increase in velocity had a similar effect. A comparative assessment among Figures 3a, 3b and 3c reveals that a reduction of wheel load resulted in a decrease in available drawbar pull energy. These phenomena are attributed to: 1) increase of velocity requires greater effort to be put on tractive characteristic of the vehicle (Eq. 3), 2) increased slippage (as a source of energy waste) results in greater available energy. Furthermore, slippage and drawbar pull have linear effect within the range of 0-15% and 3) increased wheel load leads to better interaction between tire and soil and thus increases the available drawbar pull energy. The aforementioned interpretations are compatibile with the literature [9, 24,25].

ANFIS implementations with various structures of MFs implied that triangular MF with three MFs outperformed other tested structures as tabulated in Table 3. Furthermore, it is deducible that the aforementioned ANFIS structure with the hybrid method of the gradient descent and the least-squares method to find optimal learning parameters have yielded the highest quality solutions to the corresponding problem when compared to the other tested configurations (Table 3). As can be seen, the outperforming model yielded MSE and R^2 values of 0.00236 and 0.995, respectively. Response surface curves of interactions between input parameters related to the outdone ANFIS model are illustrated in Figs. 4-6. These figures are dedicated to the interaction between velocity and wheel load, the interaction between velocity and slippage and the interaction between wheel load and slippage, respectively. The trends elucidated in Figs. 4-6 are compatible with the trends of experimental data demonstrated in Fig. 3. Hence, the same abovementioned interpretations for the trends of DPE variations with respect to the input parameters are valid for the DPE variations in Figs. 4-6. Fig. 7 shows the assessment of the applied rules in the ANFIS model for the DPE parameter. The typified value of the objective parameter is also depicted in Fig. 7 at the example averaged multitudes of different input parameters. The fitting line is given as $y = ax + b$ for the DPE parameter where the determined value for a is closer to 1 for ANFIS model and b is closer to 0 (Fig. 8). The coefficient of determination value of 0.995 for DPE parameter was obtained. These satisfactory results confirm the promising ability of ANFIS-based modeling the DPE parameter and its appilicability in various soil-wheel interaction parameters.

5. Concluding remarks

The objective was to assess the potential of ANFIS technique for prognostication of the drawbar pull energy of driving wheels. The data were obtained through a soil bin tire testing facility at three levels of wheel load, three levels of tire slippage and three levels of velocity with three replications forming a total of 81 data points. Various ANFIS MFs were tested to discover the supervised ANFIS-based models for the objective parameters. On the basis of statistical performance criteria of MSE and R^2, it was found that triangular membership function (trimf) configuration was found to denote MSE and R^2 values of 0.00236 and 0.995, respectively. It was discovered that increased slippage led to an increase in drawbar pull energy where increase of velocity had the similar effect. Also it is concluded that a reduction of wheel load resulted in a decrease in available drawbar pull energy.

References

[1] Burt EC, Lyne PW, Meiring P, Keen JF. Ballast and inflation effect on tyre efficiency. Trans ASAE 1983;26(5):1352–4.

[2] Elwaleed A.K., Yahya A., Zohadie M., Ahmad D., Kheiralla A.F. Net traction ratio prediction for high-lug agricultural tyre. Journal of Terramechanics 43 (2006) 119–139

[3] Shmulevich, I. Mussel, U. Wolf D. The effect of velocity on rigid wheel performance. Journal of Terramechanics. 1998; 35(3): 189-207.

[4] Schreiber, M., & Kutzbach, H. D. (2008). Influence of soil and tire parameters on traction. Research in Agricultural Engineering, 54, 43-49.

[5] Taner, A., Çarman K. (2012). Prediction of tire tractive performance by using artificial neural networks, Mathematical and Computational Applications; 17 (3): 182-192

[6] Kawase, Y., Nakashima, H., & Oida, A. (2006). An indoor traction measurement system for agricultural tires. Journal of Terramechanics, 43(3), 317-327.

[7] Zoz, F.M., R.D. Grisso. 2003. Traction and Tractor Performance. ASAE distinguished lecture series No.27. ASAE, ST Joseph, MI, 49085-9659, USA.

[8] Schreiber M., Kutzbach H.D., Comparison of different zero-slip definitions and a proposal to standardize tire traction performance, Journal of Terramechanics, 44(1) 2007, 75-79

[9] Pytka, J., Dąbrowski, J., Zając, M., & Tarkowski, P. (2006). Effects of reduced inflation pressure and vehicle loading on off-road traction and soil stress and deformation state. Journal of Terramechanics, 43(4), 469-485.

[10] Degirmencioglu, A., & Way, T. R. (2004). Tractive performance comparisons of radial-ply and bias-ply agricultural tractor drive tires. Agricultural Engineering, 10(1-4), 1-8.

[11] Taghavifar, H., Mardani, A., Taghavifar, L., A hybridized artificial neural network and imperialist competitive algorithm optimization approach for prediction of soil compaction in soil bin facility. Measurement (2013); 46(8); 2288-2299.

[12] Taghavifar, H.,Mardani, A., Karim-Maslak, H., Kalbkhani, H. Artificial Neural Network estimation of wheel rolling resistance in clay loam soil. Applied Soft Computing (2013): 13(8); 3544-3551

[13] Taghavifar, H., & Mardani, A. (2014). Use of artificial neural networks for estimation of agricultural wheel traction force in soil bin. Neural Computing and Applications, *24*(6), 1249-1258.

[14] Taghavifar, H., & Mardani, A. (2013). A knowledge-based Mamdani fuzzy logic prediction of the motion resistance coefficient in a soil bin facility for clay loam soil. Neural Computing and Applications, *23*(1), 293-302.

[15] Taghavifar, H., & Mardani, A. (2014). Fuzzy logic system based prediction effort: A case study on the effects of tire parameters on contact area and contact pressure. Applied Soft Computing, *14*, 390-396.

[16] Cross, M., Ellery, A., & Qadi, A. (2013). Estimating terrain parameters for a rigid wheeled rover using neural networks. Journal of Terramechanics, *50*(3), 165-174.

[17] Taghavifar, H., & Mardani, A. (2014). A comparative trend in forecasting ability of artificial neural networks and regressive support vector machine methodologies for energy dissipation modeling of off-road vehicles. Energy, *66*, 569-576.

[18] Taghavifar, H., & Mardani, A. (2014). Applying a supervised ANN (artificial neural network) approach to the prognostication of driven wheel energy efficiency indices. Energy, *68*, 651-657.

[19] Taghavifar, H., Mardani, A., & Karim-Maslak, H. (2014). Multi-criteria optimization model to investigate the energy waste of off-road vehicles utilizing soil bin facility. Energy, 73, 762-770.

[20] Ullah, N., & Choudhury, P. (2013). Flood Flow Modeling in a River System Using Adaptive Neuro-Fuzzy Inference System. Environmental Management and Sustainable Development, *2*(2), 54-68.

[21] Srinivas, Y., Raj, A. S., Oliver, D. H., Muthuraj, D., & Chandrasekar, N. (2012). Estimation of subsurface strata of earth using Adaptive Neuro-Fuzzy Inference System (ANFIS). Acta Geodaetica et Geophysica Hungarica, 47(1), 78-89.

[22] Jang, J. S. (1993). ANFIS: adaptive-network-based fuzzy inference system.*Systems, Man and Cybernetics, IEEE Transactions on*, *23*(3), 665-685.

[23] Karaağaç Bağdagül, İnal Melih, Deniz Veli, Predicting optimum cure time of rubber compounds by means of ANFIS, Materials & Design, 35, 2012; 833-838

[24] Taghavifar, H., & Mardani, A. (2013). Investigating the effect of velocity, inflation pressure, and vertical load on rolling resistance of a radial ply tire. *Journal of Terramechanics*, *50*(2), 99-106.

[25] Šmerda, T., Čupera, J. (2010). Tire inflation and its influence on drawbar characteristics and performance–Energetic indicators of a tractor set. Journal of Terramechanics, 47(6), 395-400

Figure Captions:

Figure 1- Left side view of the single wheel tester on the soil bin. L-shaped frame is the frame having one segment composed of the two vertical members forward of the test tire and the other segment composed of the horizontal structure above the test tire.

Figure 2- Adaptive neuro-fuzzy inference system configuration

Figure 3- Experimental drawbar pull energy variation with respect to increased slippage at different velocities of 0.8, 1 and 1.2 m/s at a) wheel load of 2 kN, b) wheel load of 3 kN and c) wheel load of 4 kN

Figure 4- 3D surface curves of drawbar pull energy as affected by interactions of velocity and wheel load

Figure 5- 3D surface curves of drawbar pull energy as affected by interactions of velocity and slippage

Figure 6- 3D surface curves of drawbar pull energy as affected by interactions of wheel load and slippage

Figure 7- ANFIS rule viewer and rules of the drawbar pull energy prediction model

Figure 8- The scatterplot of ANFIS predicted values versus actual values

Table legends:

Table 1
Summary of experiment conducted

Independent Parameters			Dependent Parameter
Wheel Load (kN)	Slippage (%)	Velocity (m/s)	
2	8	0.8	
3	12	1	Drawbar pull energy (kJ)
4	15	1.2	

Table 2
Soil constituents and measured physical properties

Item	Value
Sand (%)	34.3
Silt (%)	22.2
Clay (%)	43.5
Bulk density (kg/m^3)	2360
Angle of internal friction (°)	32
Cone Index (kPa)	700

Table 3

The characteristics of the best structure of developed ANFIS architectures; DPE: Drawbar pull energy

Item	Type of MF		Number of MF		Learning method	MSE for DPE	R^2 for DPE
	Input	Output	Input	Epoch			
ANFIS1	dsigmf	Linear	3,3,3	50	Hybrid	0.01428	0.953
ANFIS2	Gbellmf	Linear	3,3,3	50	Hybrid	0.01243	0.964
ANFIS3	Gbellmf	Linear	5,3,5	50	Hybrid	0.00892	0.942
ANFIS4	Pimf	Linear	3,3,3	50	Hybrid	0.01727	0.933
ANFIS5	**Trimf**	**Linear**	**3,3,3**	**50**	**Hybrid**	**0.00236**	**0.995**
ANFIS6	Trimf	Linear	4,4,4	50	Hybrid	0.00681	0.981
ANFIS7	Tramf	Linear	3,3,3	50	Hybrid	0.01245	0.977
ANFIS8	Gaussmf	Linear	3,3,3	50	Hybrid	0.01897	0.957
ANFIS9	Gaussmf	Linear	3,4,5	50	Hybrid	0.00962	0.985
ANFIS10	Pimf	Linear	3,5,3	50	Hybrid	0.01348	0.956
ANFIS11	Tramf	Linear	4,4,4	50	Hybrid	0.01699	0.978
ANFIS12	dsigmf	Linear	4,4,4	50	Hybrid	0.01728	0.969

Illustration number: **Figure 1**

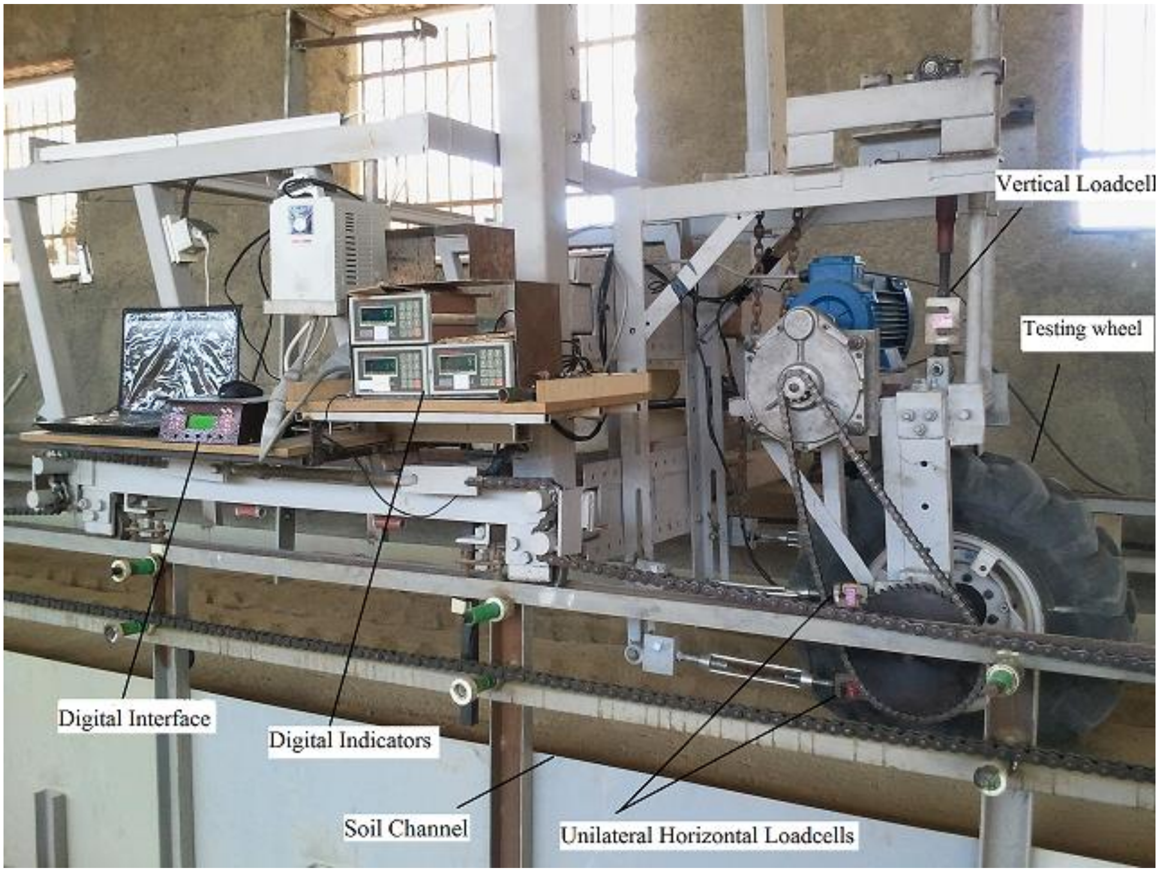

This is the pre-print version of the paper published by Journal of Energy

Illustration number: **Figure 2**

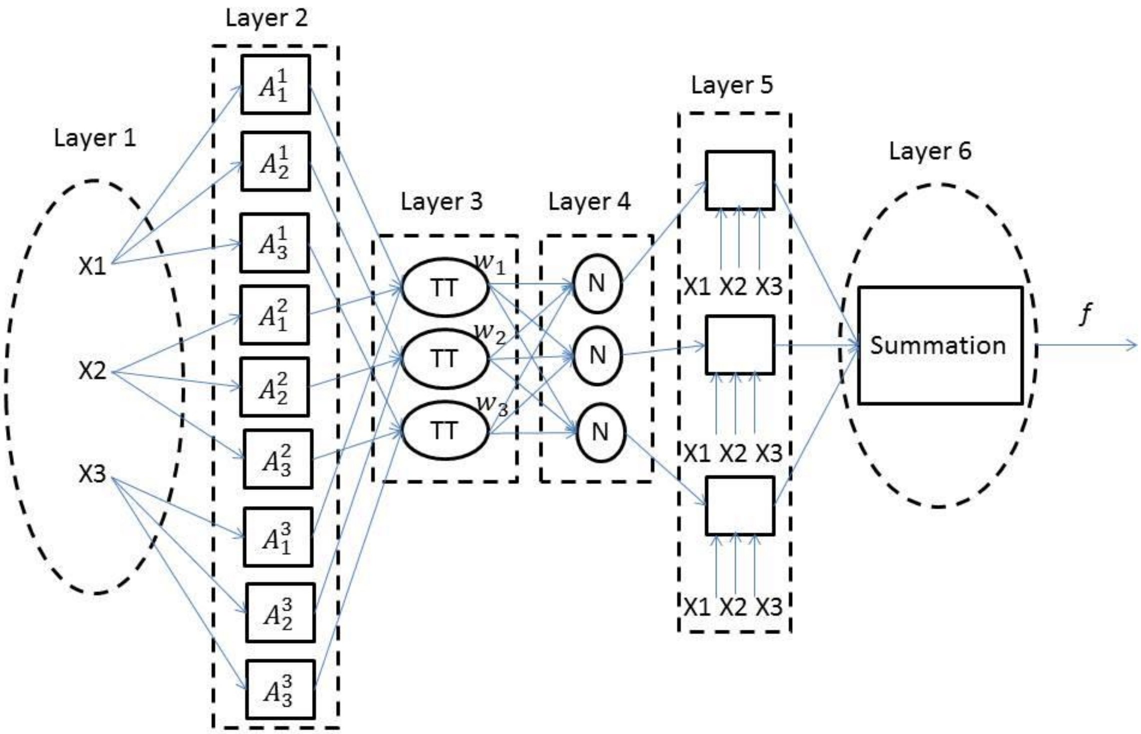

Illustration number: **Figure 3 (a)**

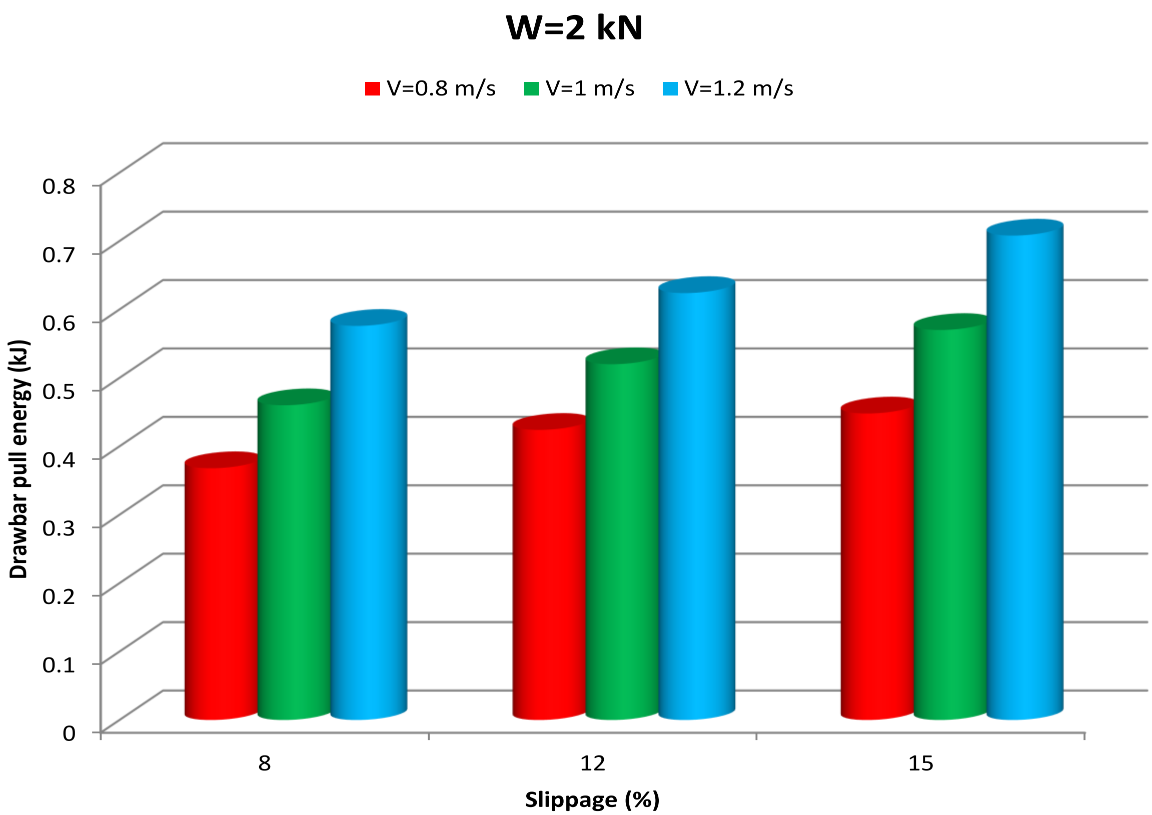

Illustration number: **Figure 3 (b)**

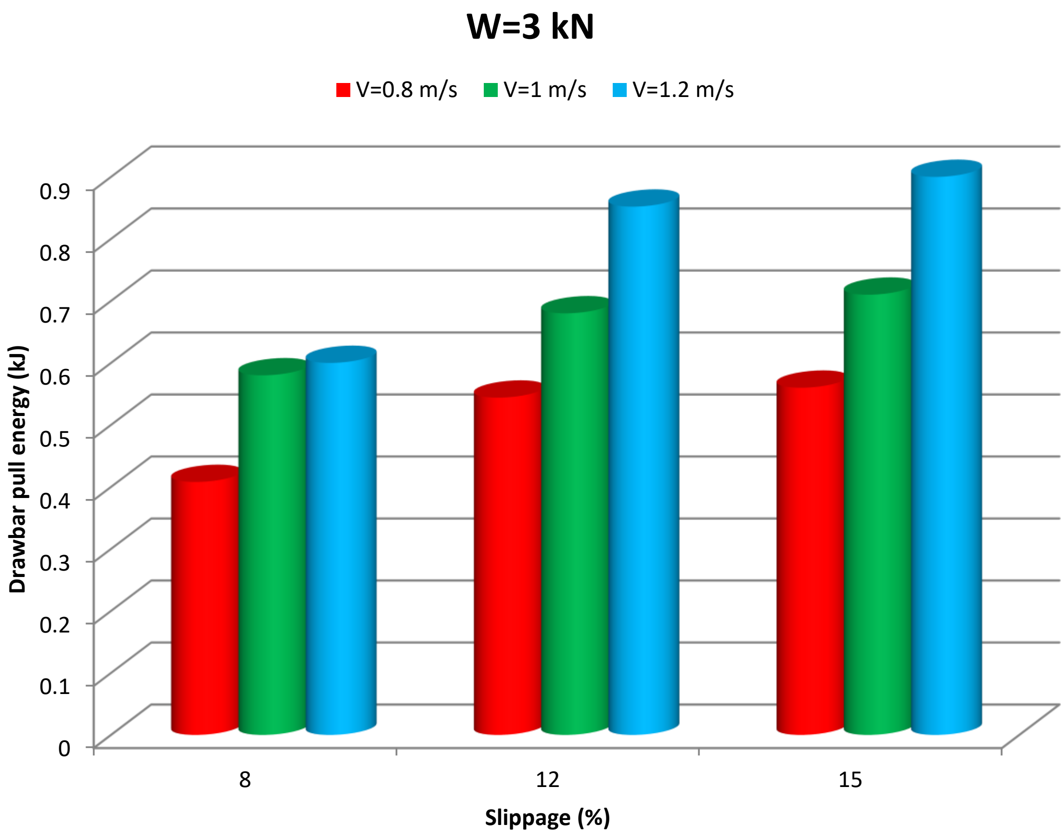

This is the pre-print version of the paper published by Journal of Energy

Illustration number: **Figure 3 (c)**

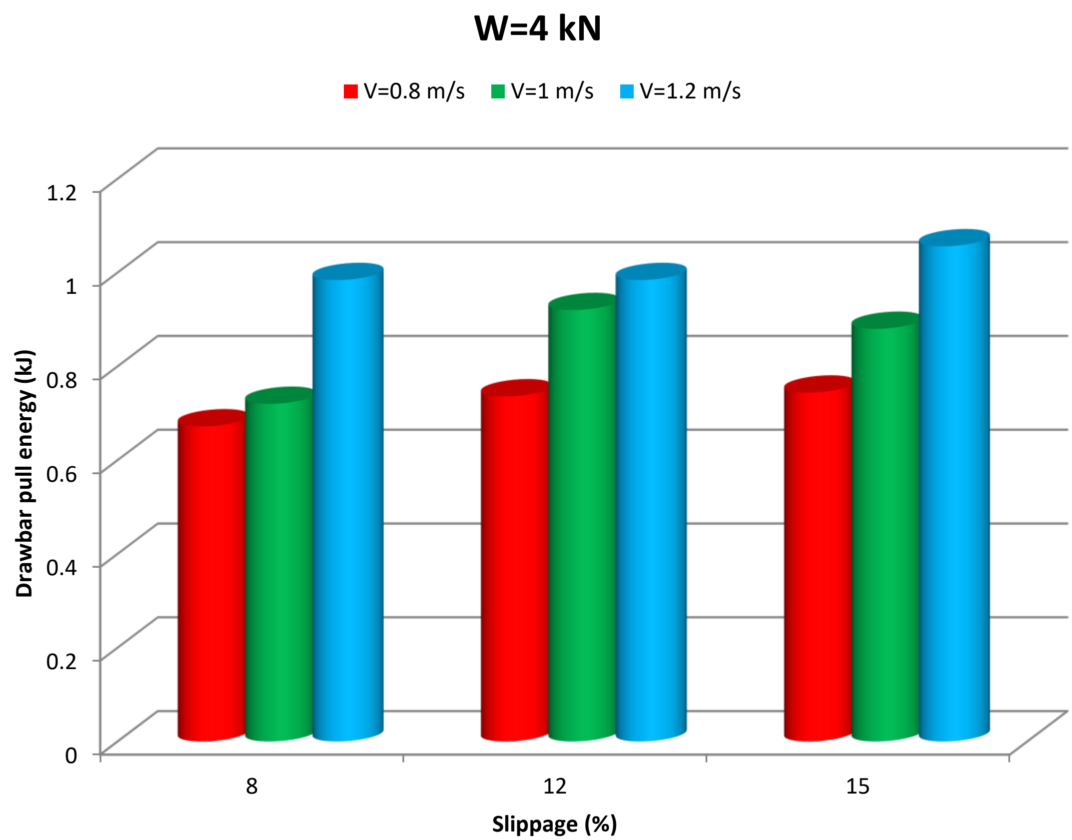

Illustration number: **Figure 4**

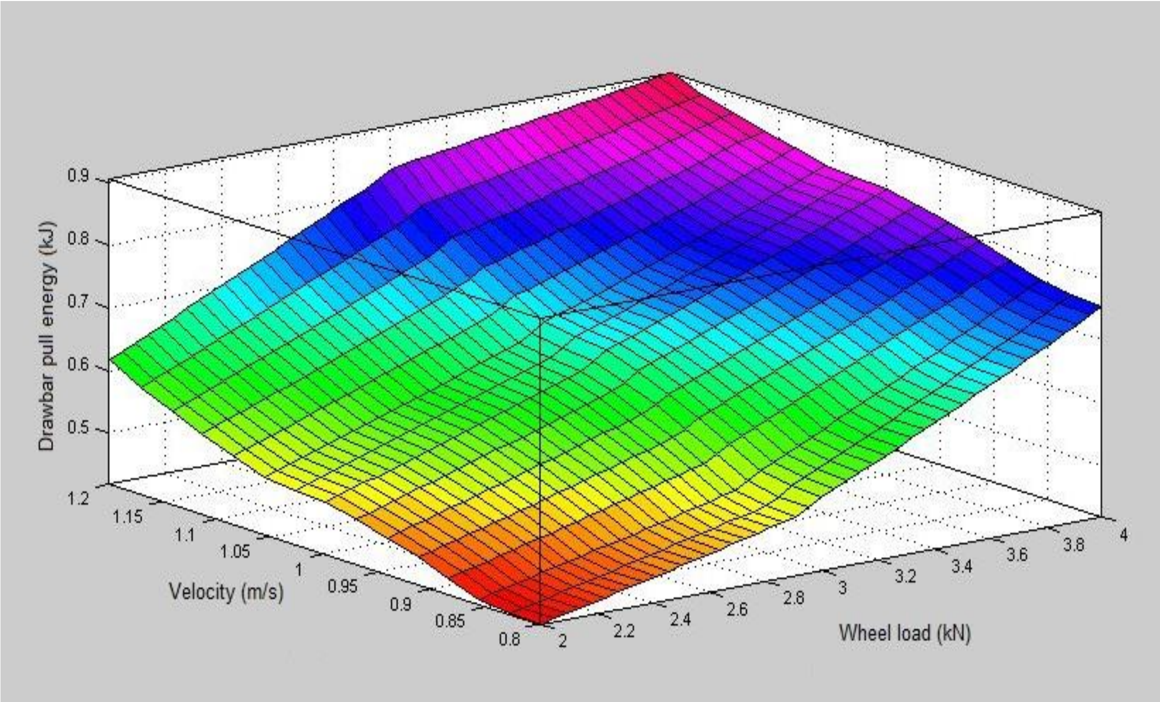

Illustration number: **Figure 5**

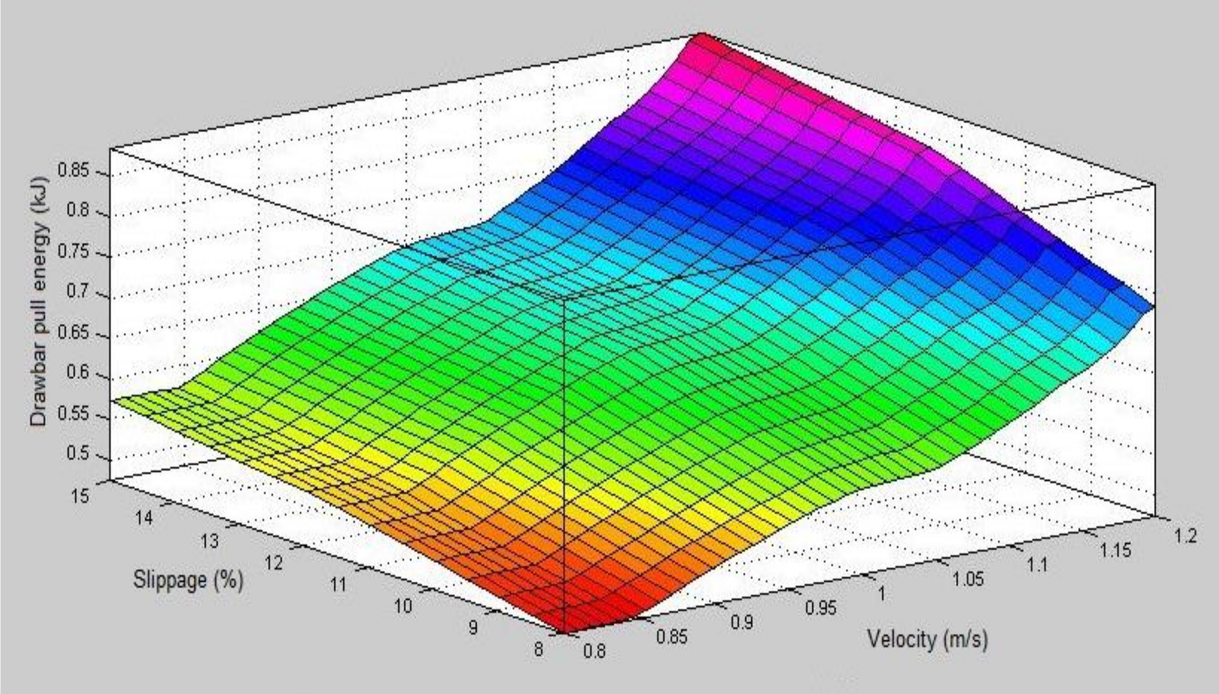

Illustration number: **Figure 6**

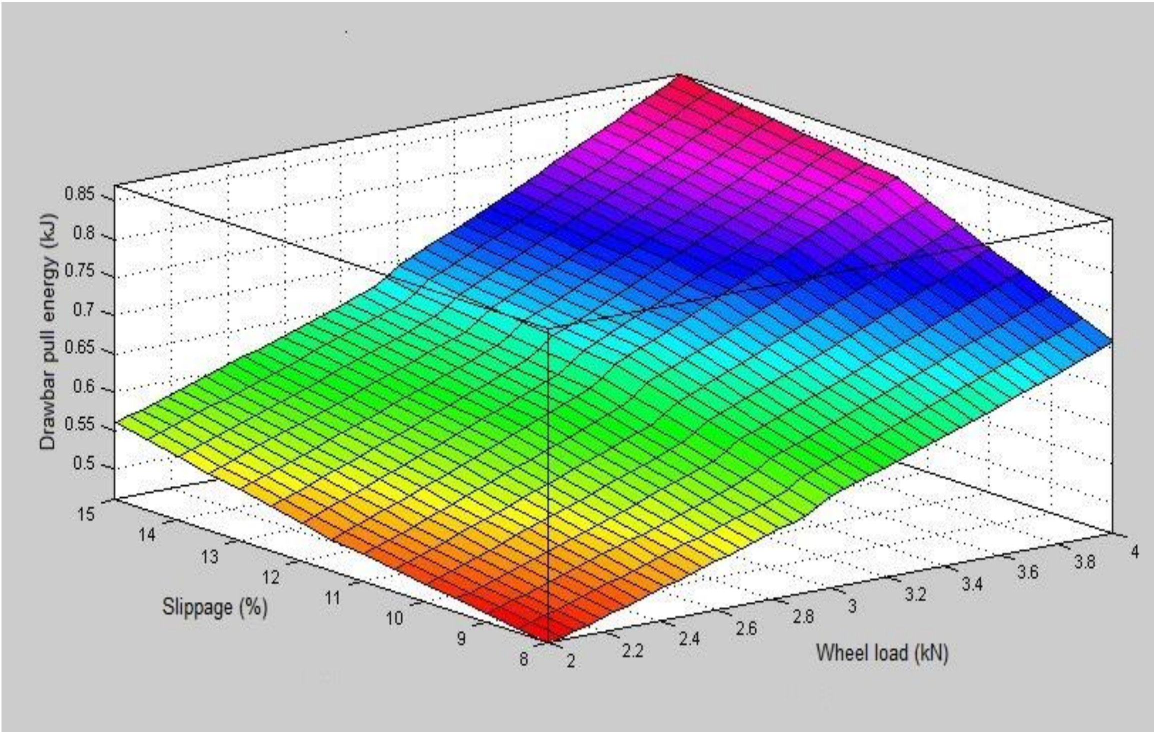

Illustration number: **Figure 7**

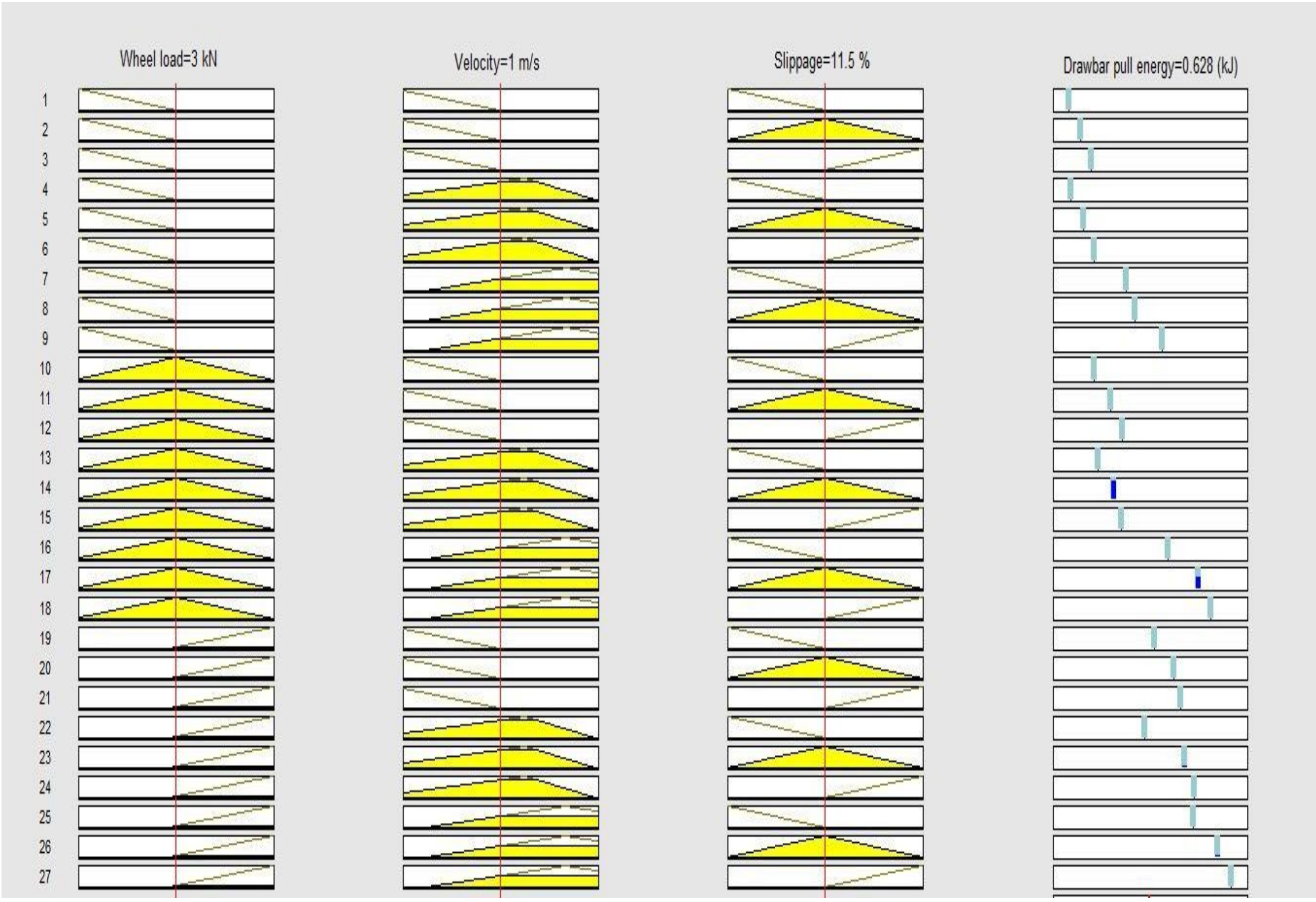

Illustration number: **Figure 8**